BNL-203498-2018-TECH

EIC/60

On the effects of detector solenoids on n0 in RHIC and eRHIC

F. Méot

April 2018

Collider Accelerator Department

Brookhaven National Laboratory

U.S. Department of Energy

USDOE Office of Science (SC), Nuclear Physics (NP) (SC-26)

DISCLAIMER

On the effects of detector solenoids on $\vec{n}_0$ in RHIC and eRHIC

F. Méot, E.-C. Aschenauer, H. Huang, J.C. Webb
BNL, Upton, NY 11973

April 6, 2018

Abstract

Two effects, in RHIC, from STAR solenoid and from a model of sPHENIX detector solenoid, are reviewed based on tracking simulations: a change in the stable spin precession direction $\vec{n}_0$ around the ring, and coupling. The method can be applied, *mutatis mutandis*, to eSTAR, sPHENIX and BeAST detector solenoids in A- and e-eRHIC.

eRHIC Note 60
BNL C-AD

Contents

1 Introduction

A possible contribution of STAR solenoid to the observed tilt of RHIC spin $\vec{n}_0$ vector is investigated, as a follow on of earlier investigations [1, 2]. Run 17 optics is used for RHIC modeling [3]. While we are there, we also take a look at the amount of coupling introduced by STAR. Note that there is no local coupling compensation in real-life RHIC (neither in the present RHIC model).

This brief study is taken as an opportunity to comment (as briefly) on some aspects of the effects of the IR6 and IR8 solenoid detectors (namely, taking eSTAR and sPHENIX typical parameters) in eRHIC context [4].

2 RHIC lattice including STAR solenoid

2.1 RHIC optics

Field maps for the STAR solenoid are available over a great volume, typically up to a radius $\mathrm{R} = 2.22$ m, and extend longitudinally up to $\Delta\mathrm{z} = \pm 8.1$ m centered at IP6. As we are concerned here about RHIC beam optics and polarization, which means paraxial behavior, we use the on-axis field map data (for the record: so-called "STAR_FIELD_8m.20170305.dat" file). It would be possible to handle the latter directly using zgoubi's 'BREVOL' field map routine, however we choose instead to use these field data for generating the *ad hoc* parameters for analytical modeling of the magnet with zgoubi's 'SOLENOID' [5]. The solenoid model has a coil length L, a reference radius R_0 and an asymptotic field $\mathrm{B}_\infty = \mu_0 \mathrm{NI}/\mathrm{L}$ (*i.e.*, $\int_{-\infty}^{\infty} \mathrm{B_z}(\mathrm{z},\mathrm{r})\mathrm{dz} = \mu_0 \mathrm{NI},\ \forall \mathrm{r} < \mathrm{R}_0$), wherein $\mathrm{B_z}$=longitudinal field component, NI= number of ampere-Turns, $\mu_0 = 4\pi 10^{-7}$, and can be written

$$\mathrm{B_z}(\mathrm{z},\mathrm{r}=0) = \frac{\mathrm{B}_\infty}{2}\left[\frac{\mathrm{L}/2-\mathrm{z}}{\sqrt{(\mathrm{L}/2-\mathrm{z})^2+\mathrm{R}_0^2}} + \frac{\mathrm{L}/2+\mathrm{z}}{\sqrt{(\mathrm{L}/2+\mathrm{z})^2+\mathrm{R}_0^2}}\right] \tag{1}$$

with $\mathrm{z} = \mathrm{r} = 0$ taken at the center of the solenoid. This model assumes that the coil thickness is small compared to the mean radius R_0. In this model, the magnetic length is

$$\mathrm{L_{mag}} \equiv \frac{\int_{-\infty}^{\infty} \mathrm{B_z}(\mathrm{z},\mathrm{r}<\mathrm{R}_0)\mathrm{dz}}{\mathrm{B_z}(\mathrm{z}=\mathrm{r}=0)} = \mathrm{L}\sqrt{1+\frac{4\mathrm{R}_0^2}{\mathrm{L}^2}} > \mathrm{L} \tag{2}$$

with in addition $\mathrm{B_z}(\mathrm{z}=\mathrm{r}=0) = \mathrm{B}_\infty/\sqrt{1+\frac{4\mathrm{R}_0^2}{\mathrm{L}^2}}$. By fitting Eq. 1 to the on-axis field data, with variables L, R_0, B_∞, one gets

$$\mathrm{L} = 6.93172\ \mathrm{m},\ \ \mathrm{R} = 0.6633\ \mathrm{m},\ \ \mathrm{B}_\infty = -5.174\ \mathrm{T}\ \text{ yielding } \int_{-\infty}^{\infty} \mathrm{B_z}(\mathrm{z},\mathrm{r}=0)\mathrm{dz} = \mu_0 \times \mathrm{NI} = -3.587\,\mathrm{T\,m},$$

As shown in Fig. 1, Eq. 1 with these data gives the closest match to STAR field map data. Note, tracking-wise: at all (z,r), the necessary field and derivatives for tracking are extrapolated from Eq. 1, following the methods described in [5].

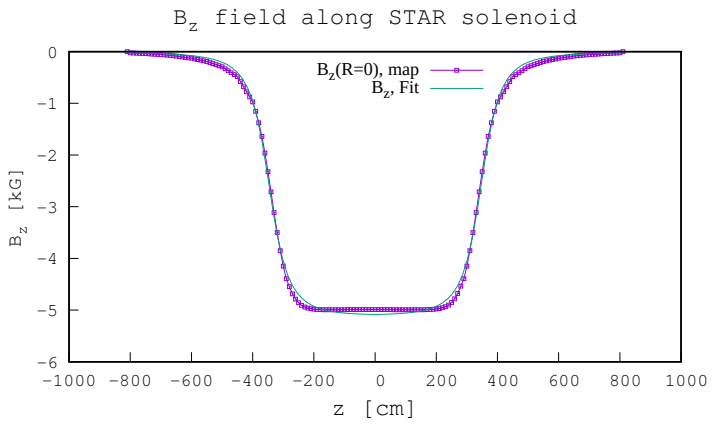

Figure 1: Magnetic field along STAR axis, using its field map (markers) or using zgoubi's semi-analytical SOLENOID model (solid line).

THE FIGURES ON THIS PAGE ARE COPIED FROM TECH. NOTE C-A/AP/590, FOR REFERENCE
Origin of ring is taken at IP6.
Snake settings are taken nominal: axes at $\phi = \mp 45$ deg. in respectively snake 1, 2, and $\mu = 180$ deg spin rotation.

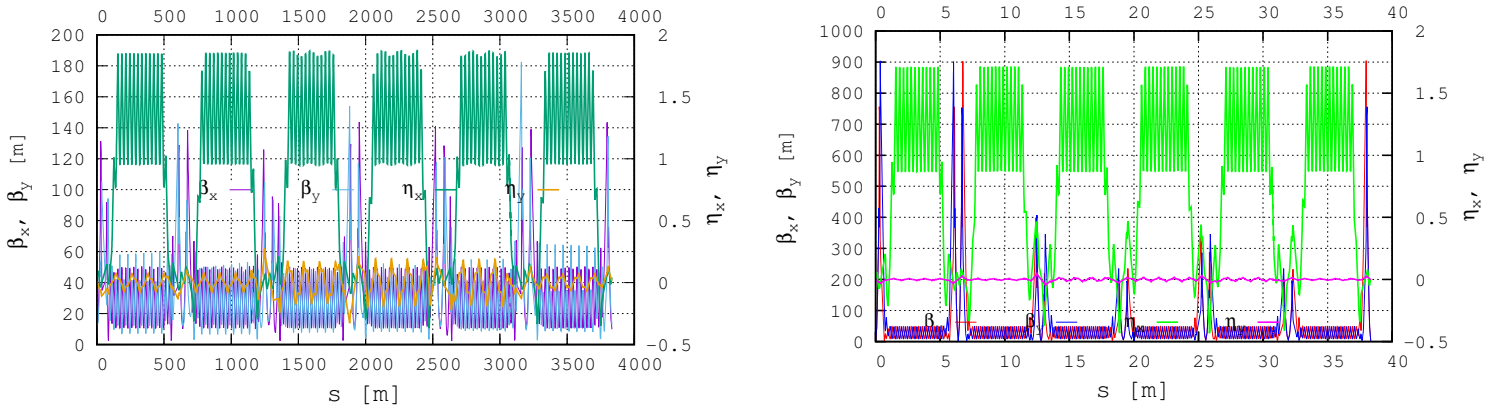

Figure 2: Optical functions in this model, at injection (left) and store (right) (figures respectively (20) and (30) in [6]). They include the two snakes using their 3D OPERA field maps. These cause of a slight perturbation in the vertical focusing, at injection, compared to a snake-free optics.

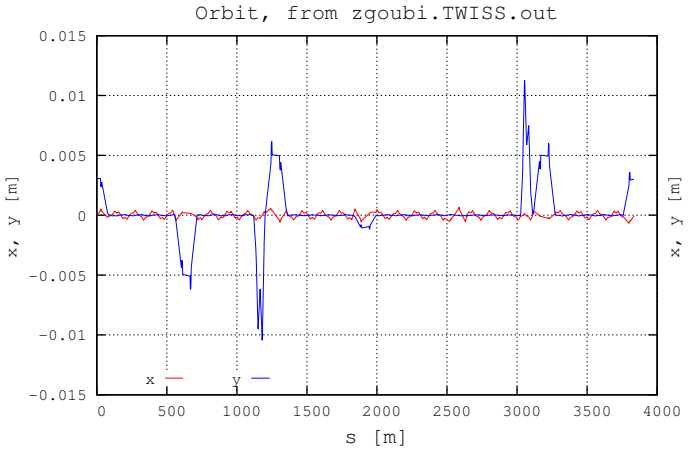

Figure 3: H and V orbits in RHIC at injection, Run 17 optics model. Snakes are theoretical spin rotators here - not field maps, however the local vertical orbit bumps at the snakes are accounted for, as can be seen right upstream of IP10 and of IP4.

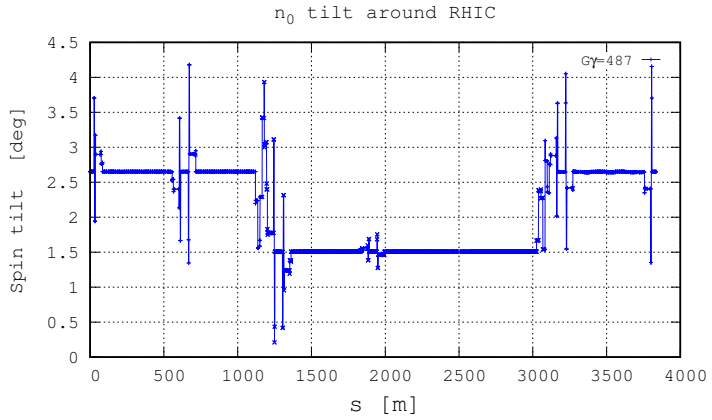

Figure 4: Vertical tilt of $\vec{n}_0$ around RHIC at injection. Note that when using field maps to simulate the snakes, local $\vec{n}_0$ tilt extrema of about 14 deg appear at the two snakes, they are absent here as SPINR does not introduce any orbital effect [6].

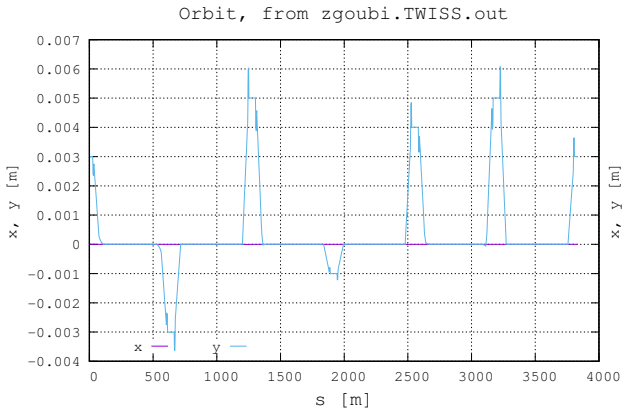

Figure 5: H and V orbits in RHIC at store, Run 17 optics model. Snakes are theoretical spin rotators here - not field maps. The vertical orbit perturbations by the snakes are quasi-zero at store (they are taken exactly zero in the zgoubi model).

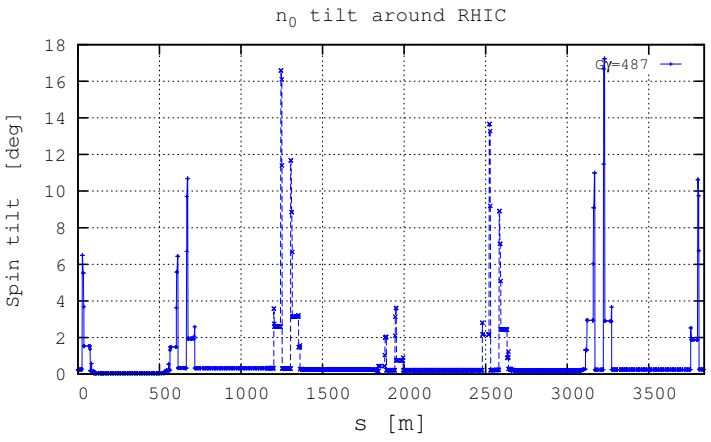

Figure 6: Vertical tilt of $\vec{n}_0$ around RHIC at store. These tilts occur at the rise and fall of the vertical separation bumps at IPs.

Three remarks to conclude on STAR and RHIC modeling :

(i) The field model does not feature the plateau seen in the data, this is because it does not account for any end field clamp effect which would sharpen the field fall-offs. However this is good enough for our paraxial studies, where essentially the field integral matters, rather than the precise field shape.

(ii) STAR is slightly shifted with respect to the RHIC axis, and slightly tilted as well (and even more so in the eRHIC design, where detector magnets are aligned on the electron beam axis). However, as the simulations will show (next sections), coupling and $\vec{n}_0$ tilt induced by the detector solenoid amount only to perturbations, thus these additional shift and tilt amount to perturbations on a perturbation and we chose here to ignore them and will treat STAR as perfectly aligned at IP6.

(iii) We use here the very RHIC model investigated in detail in C-A/AP/590 [6], and simulate the two snakes using a pure spin rotator, no orbital effect (zgoubi's 'SPINR' [5]). In these conditions, free of detector solenoid, the same as in C-A/AP/590 including the vertical orbit separation bumps at IPs, $\vec{n}_0$ undergoes a noticeable perturbation as seen in Figs. 4, 6 (copied from [6] for reference).

2.2 $\vec{n}_0$ in the presence of STAR

Fig. 7 summarizes how much the STAR solenoid changes the tilt of $\vec{n}_0$ around RHIC, at injection and at store. At injection $\vec{n}_0$ tilt is weak *ab initio*, below $\sim 4.5^o$, and with STAR it stays below $\sim 7^o$ (in terms of polarization: $\cos(7^o)$ =99.2%, still a small effect). At store the effect of STAR is negligible compared to the substantial $10\sim 17^o$ effect of the vertical orbit separation bumps in the IRs (polarization-wise: $\cos(10\sim 16^o) \approx 98.5\sim 95.6\%$).

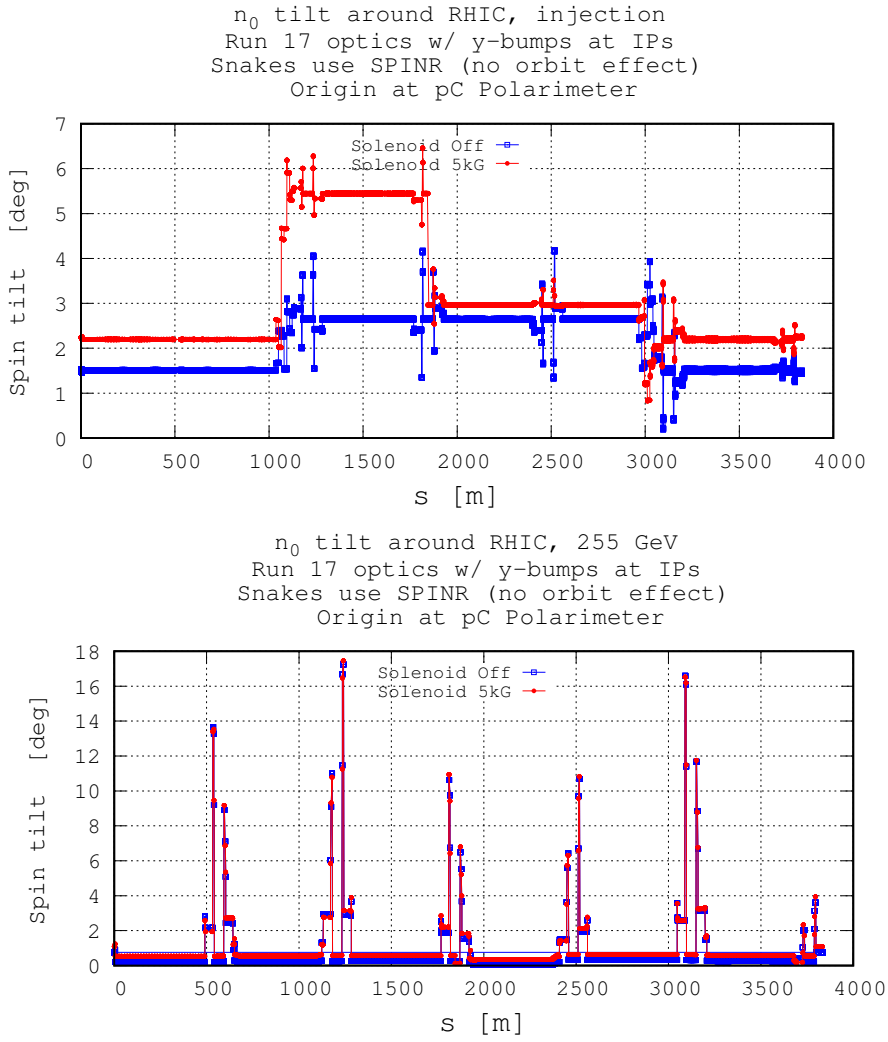

Figure 7: Vertical tilt of $\vec{n}_0$ around RHIC at injection (top) and store (bottom). Origin of the lattice here is taken at the pC polarimeter (located about 70 m from IP12, downstream clockwise). Snake angles are nominal, rotation axis at $\phi = \mp 45$ deg. in respectively snake 1, 2, and spin rotation $\mu = 180$ deg. The red curves are in the presence of the STAR solenoid. The blue curves are for the STAR-free lattice as displayed in Figs. 4 (injection) and 6 (store), with just a different origin of the lattice.

2.3 While we are here: coupling from STAR

We quantify the coupling at injection and at store, by a closest tune approach scan. This is summarized in Fig. 8. The coupling amounts to respectively $\approx 1.5\,10^{-2}$ and $\approx 5\times10^{-4}$ at injection and store (the effect is included of course, in the case of $\vec{n}_0$ results in Fig. 7). There is no other source of coupling in the present model (snakes are pure spin tools here, no orbital effect).

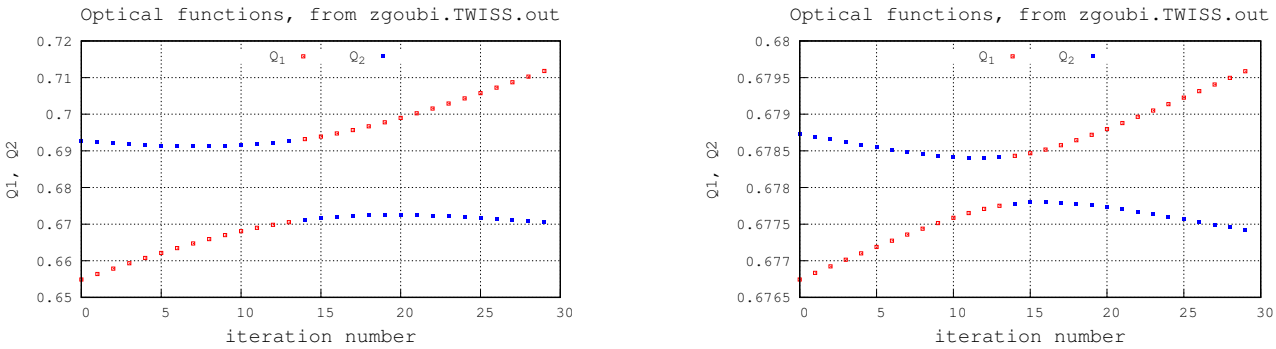

Figure 8: Closest approach tune scans in the vicinity of the nominal working point, in the presence of STAR. Left : at injection (unperturbed tunes are Qx/Qy=28.6895/29.6796). Right : at store (unperturbed tunes are Qx/Qy=28.685/29.675).

3 Case of sPHENIX solenoid parameters

3.1 RHIC optics

The same model in zgoubi as for STAR is used for sPHENIX (Eqs. 1, 2) with now

$$\mathrm{B}_\infty = 1.4\,\mathrm{T} \quad \text{and} \quad \mathrm{L} = 4\,\mathrm{m},$$

$$\int_{-\infty}^{\infty} \mathrm{B_z(z, r = 0)dz} = 5.6\,\mathrm{T\,m}$$

RHIC snakes are as in the earlier simulations, axes at $\phi = \mp 45$ degree and spin rotation $\mu = 180$ degree. RHIC orbits including vertical separation bumps at IPs are as shown in Fig. 3 (injection) and Fig. 5 (extraction). The optical functions are slightly perturbed when inserting the solenoid in the lattice. However in spite of a greater field integral the perturbation is still weak, thus the optics is left as it is, Fig. 9.

3.2 $\vec{n}_0$

Fig. 10 summarizes how much sPHENIX solenoid changes the tilt of $\vec{n}_0$ around RHIC, at injection and at store. At injection $\vec{n}_0$ tilt is weak *ab initio*, below 6.5^o about, and sPHENIX leaves it below 6^o (in terms of polarization: $\cos(6^\mathrm{o})$ =99.5%, still a small effect). At store sPHENIX increases the maximum tilt by less than 1^o, to below 18^o ($\cos(18^\mathrm{o}) \approx 0.951$).

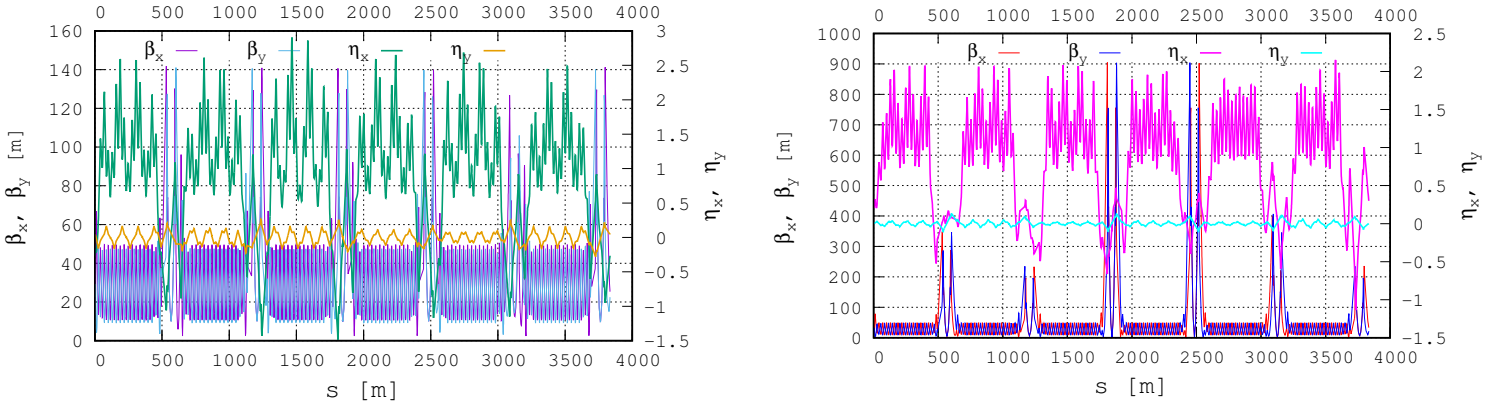

Figure 9: Optical functions, uncorrected, under the effect of sPHENIX, at injection (left) and store (right).

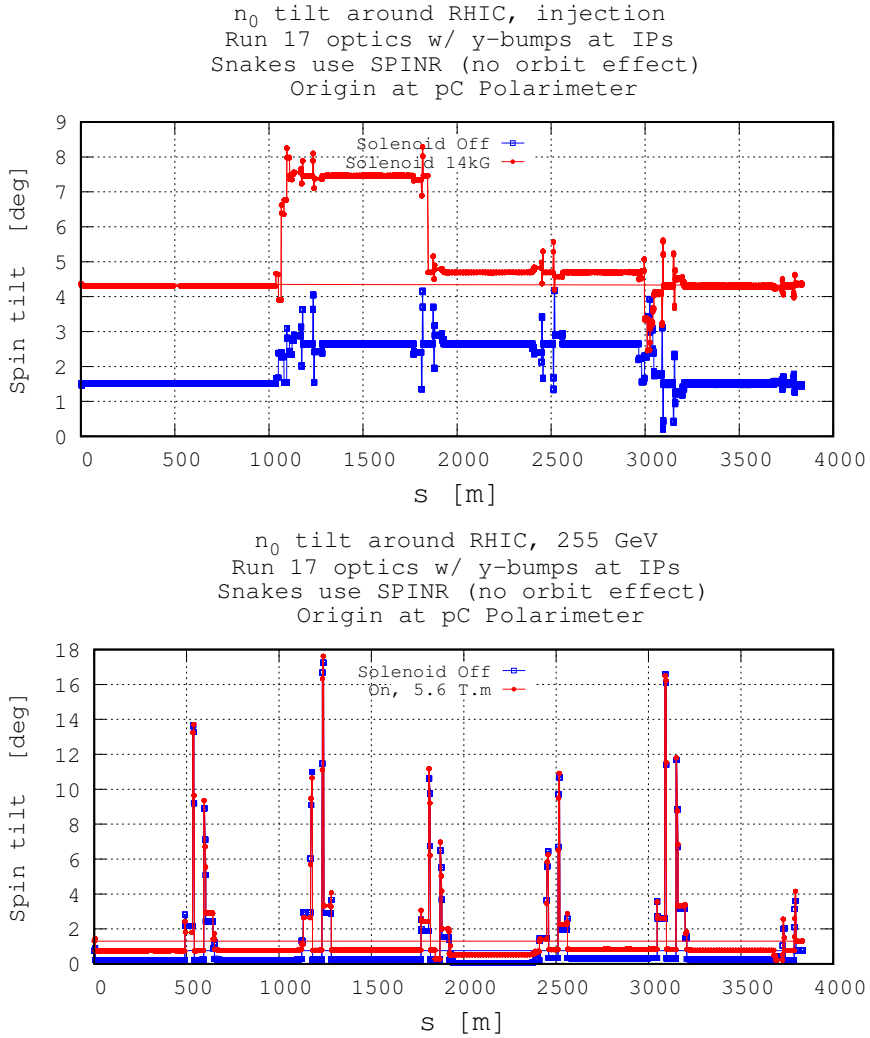

Figure 10: Vertical tilt of $\vec{n}_0$ around RHIC at injection (top) and store (bottom). Origin of the lattice here is taken at the pC polarimeter (70 m away from IP12). Snake angles are nominal, rotation axis at $\phi = \mp 45$ deg. in respectively snake 1, 2, and spin rotation $\mu = 180$ deg. The red curves are for the sPHENIX case. The blue curves are for the solenoid-free lattice, as displayed in Figs. 4 (injection) and 6 (store), with just a different origin of the lattice.

3.3 Coupling

The closest approach scan is summarized in Fig. 11. The coupling amounts to respectively $\approx 2\,10^{-2}$ and $\approx 10^{-3}$ at injection and store respectively. The effect is included of course in the $\vec{n}_0$ results of Fig. 10.

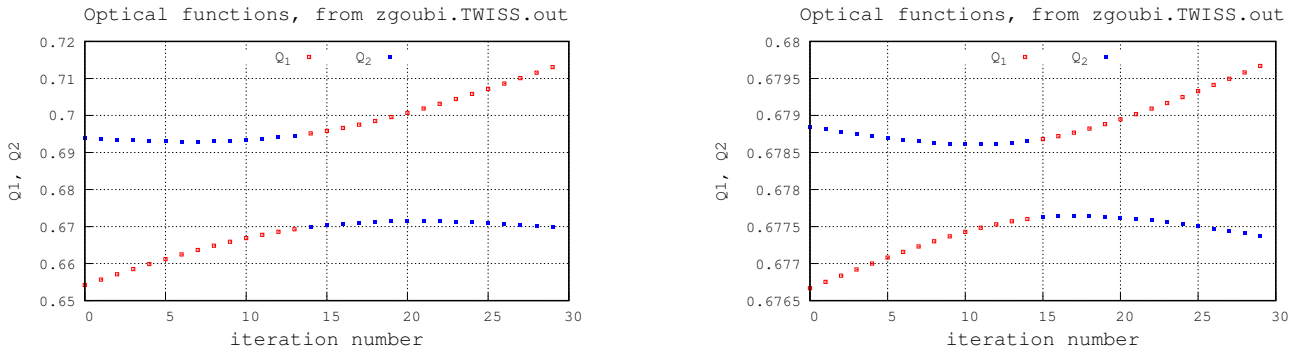

Figure 11: Closest approach tune scans in the vicinity of the nominal working point, in the presence of sPHENIX. Left : at injection (unperturbed tunes are Qx/Qy=28.6895/29.6796). Right : at store (unperturbed tunes are Qx/Qy=28.685/29.675).

4 Regarding eRHIC

The effect of the detector solenoid on synchrotron-radiation induced spin diffusion in the eRHIC electron storage ring (e-eRHIC) has recently been assessed [4] using the sPHENIX solenoid data given in Tab 1. Typical results are given in Tab. 1 as an illustration.

The very method discussed above (using field maps to generate a semi-analytical model closer to actual magnetic field shape) can be applied, *mutatis mutandis* in both A- and e-eRHIC, for all three types of detector solenoids foreseen, BeAST, sPHENIX, eSTAR.

Table 1: Cols. 2-5: parameters of eRHIC detector solenoids, respectively length (L), diameter (Φ), central field (B_0), field integral along the solenoid axis. Col. 6: optical coupling strength at e-eRHIC (min.($|Q_1 - Q_2|$) in the vicinity of the tune diagonal). Cols. 7, 8: tune perturbation (unperturbed transverse modes are $Q_x = 0.08$, $Q_y = 0.06$). Cols. 9, 10 and 11, 12: polarization time constants (diffusion and equilibrium) obtained by tracking, respectively in the absence and in the presence of sPHENIX solenoid.

	L	Φ	B_0	$\int B\,dl$	$\Delta Q_{1,2}$	δQ_1, $\delta Q2$, absolute	w/o sol.		w sol.	
							τ_{diff}	τ_{eq}	τ_{diff}	τ_{eq}
	(m)	(m)	(T)	(Tm)		($\times 10^{-3}$)	(minute)		(minute)	
BeAST	5	3	3	15	0.021	$+23, -25$				
sPHENIX	4	2.7	1.4	5.6	0.024	$+5.4, -5.7$	58	20	20	12
eSTAR	5.0	4.5	0.5	3.6	0.025	$+2.8, -2.5$				

5 Conclusion

The main effect from the detector solenoid in RHIC, or A-eRHIC, is tilting the stable spin precession axis away from vertical. A detector solenoid magnet generates a small tilt of the precession axis, equivalent to a partial snake. For the STAR magnet at store energy 255 GeV, the partial snake strength is 0.26% (a 0.5° rotation of spins). The vertical tilt of the precession axis is negligible. At injection energy, the partial snake strength is 2.8% (rotation of spins $\sim 5°$). Even in this case, the vertical tilt of the stable precession axis is still small. The precession axis tilt in the whole RHIC hadron ring for a realistic lattice (with separation bumps and snake field map included) has been studied for STAR magnet at 25 GeV (injection) and 255 GeV [6], it can be concluded that whether the STAR solenoid magnet is on or off has very little effect on the vertical component. The same method can be applied to the BeAST solenoid magnet.

APPENDIX

A Zgoubi data file for Q-scan, STAR case

RHIC SEQUENCE :

```
Generated by MADX -> Zgoubi translator
 'OBJET'
850.14060738641490E3                                    ! 255 GeV region
5
.001 .01 .001 .01 .001 .0001
-1.41753E-03 8.48444E-04 -1.19744E-02 2.01607E-02 0. 1.  'o' ! orbit, case solenoid=-5kG

 'SCALING'
1  5
BEND
-1
850.14060738641490E+00
1
MULTIPOL
-1
850.14060738641490E+00
1
MULTIPOL HKIC VKICK
-1
850.14060738641490E+00
1
MULTIPOL QF
-1
850.140606E+00
1
MULTIPOL QD
-1
850.140605E+00
1
 'OPTIONS'
1 1
WRITE OFF

'INCLUDE'
1
pCPol2STAR.dat
'INCLUDE'
1
STAR.dat[STAR_up , :STAR_dwn , ]
'INCLUDE'
1
STAR2pCPol.dat

'OPTIONS'
1 1
WRITE ON

 'FAISCEAU'
 'SPNPRT'   MATRIX  PRINT

'MATRIX'
1  11  coupled
 'REBELOTE'
30  .1  0 1
1
SCALING 16  850.08:850.10   ! change scaling/QF
 'END'
```

SOLENOID at IP6 ('INCLUDE' STAR.dat file) :

```
STAR matrix, 255 GeV
 'OBJET'
850.14060738641490E3
5
.001 .01 .001 .01 .001 .0001
0. 0. 0. 0. 0. 1.

 'MARKER'   STAR_up
 'DRIFT'
-346.5
 'SOLENOID'
0  .soleno
693.  10. -5.  ! 5kG => field integral 3.46, a little lower than STAR's 3.59
300.    300.   ! 3 m extention allows marginal residual \int Bdl
1.  Soleno  IP6
1 0. 0. 0.
 'DRIFT'
-346.5
 'MARKER'   STAR_dwn

 'MATRIX'
1 11
 'END'
```

gnuplot_QscanFromZRes.cmd :

```
system "grep 'NU_Y = ' zgoubi.res | cat > gnuplot_temp"

 set title "Optical functions, from zgoubi.TWISS.out"    font "roman,16"   # offset 0,+.7
 set xlabel "iteration number"        font "roman,16"   # offset +4,-.5 rotate by +20
 set ylabel "Q1, Q2"             font "roman,13"   #offset -0,-1 rotate by -20
 set xtics  font "roman,12" nomirror
 set ytics  font "roman,12" nomirror      #offset 0,-.6

set key t c maxrows 1 width 4
set key font "roman, 12"  samplen 1

set grid
 plot \
      "gnuplot_temp" every ::1 u :($3) w p pt 4 ps .4 lc rgb "red" tit "Q_1"  ,\
      "gnuplot_temp" every ::1 u :($6) w p pt 5 ps .4 lc rgb "blue" tit "Q_2"

 set terminal postscript eps blacktext color enh size 8.3cm,5cm "Times-Roman" 12
 set output "gnuplot_Qscan.eps"
 replot
 set terminal X11
 unset output
pause 1
exit
```

B sPHENIX case

Same as in App. A, except for the solenoid section.

SOLENOID at IP6 ('INCLUDE' sPHENIX.dat file) :

```
sPHENIX matrix, 255 GeV
 'OBJET'
850.14060738641490E3       ! 255 GeV region
5
.001 .01 .001 .01 .001 .0001
0. 0. 0. 0. 0. 1.

 'MARKER'   sPHENIX_up
 'DRIFT'
-200.
 'SOLENOID'
0  .soleno
400.0000     3.   -14.
100.00    100.00     !  1 m extention allows marginal residual \int Bdl
1.  Soleno  IP6
1 0. 0. 0.
 'DRIFT'
-200.
 'MARKER'   sPHENIX_dwn

 'MATRIX'
1 11
 'END'
```

References

[1] Exploring a possible origin of a 14 degree y-normal spin $\vec{n}_0$ tilt at RHIC polarimeter, F. Méot, H. Huang, Tech Note BNL C-A/AP/538 (2015).

[2] Exploring a Possible Origin of an Abnormal $10 \backsim 15$ degree Spin Tilt Observed at RHIC Polarimeters, F. Méot, R. Gupta, H. Huang, V. Ranjbar, W. Schmidke, SPIN'16 Conf., Champaign, IL, USA (2016).

[3] G. Robert-Demolaize, priv. comm., BNL C-AD, 2017.

[4] Chapter 5 in eRHIC pCDR, BNL C-AD, to be released.

[5] Zgoubi Users' Guide, F. Méot, Tech. Note C-A/AP/470 (2012), Rep. BNL-98726-2012-IR. https://www.osti.gov/scitech/biblio/1062013-zgoubi-users-guide

[6] F. Méot, R. Gupta, H. Huang, V. Ranjbar, G. Robert-Demaulaize, Re-visiting RHIC snakes : OPERA fields, $\vec{n}_0$ dance, Tech. Note BNL C-A/AP/590 (2017).